

# Wake Sensing for Aircraft Formation Flight

Maziar S. Hemati,\* Jeff D. Eldredge,† and Jason L. Speyer‡  
*University of California, Los Angeles, California 90095-1597*

DOI: 10.2514/1.61114

It is well established that flying aircraft in formation can lead to improved aerodynamic efficiency. However, successfully doing so is predicated on having knowledge of the lead aircraft's wake position. Here, a wake-sensing strategy for estimating the wake position and strength in a two-aircraft formation is explored in a simplified proof-of-concept setting. The wake estimator synthesizes wing-distributed pressure measurements, taken on the trailing aircraft, by making use of an augmented lifting-line model in conjunction with both Kalman-type and particle filters. Simple aerodynamic models are introduced in constructing the filter to enable fundamental wake-sensing challenges to be identified and reconciled. The various estimation algorithms are tested in a vortex lattice simulation environment, thus allowing the effects of modeling error to be analyzed. It is found that biases in the position estimates no longer arise if a particle filter is used in place of the Kalman-type filters. Filter divergence is observed when the relative aircraft separations are held fixed. This divergent behavior can be alleviated with the introduction of relative aircraft motions, for example in the form of a cross-track dither signal.

## Nomenclature

$b$	=	wake vortex separation distance
$\tilde{b}$	=	wingspan
$c$	=	chord length
$H$	=	measurement Jacobian matrix
$K_L$	=	airfoil constant, $(1/2) c_{m_o}$
$\mathbf{k}_{cal}$	=	calibration vector
$M_k$	=	estimation covariance matrix
$m_o$	=	two-dimensional lift-curve slope
$V_y$	=	lateral velocity component
$V_z$	=	vertical velocity component
$\mathbf{v}_k$	=	measurement noise vector, $\mathcal{N}(0, V_k)$
$w_o$	=	wake-induced upwash
$\mathbf{w}_k$	=	process noise vector, $\mathcal{N}(0, W_k)$
$\mathbf{x}$	=	state vector
$y_o$	=	wake lateral coordinate
$\mathbf{z}$	=	measurement vector
$z_o$	=	wake vertical coordinate
$\alpha$	=	angle of attack
$\alpha_{l=0}$	=	two-dimensional zero-lift angle of attack
$\Gamma$	=	lifting surface strength
$\Gamma_o$	=	wake vortex strength
$\Delta C_p$	=	spanwise differential pressure coefficient
$\sigma_v$	=	measurement noise standard deviation
$\sigma_w$	=	process noise standard deviation
$\Omega_x$	=	roll rate
$\Omega_y$	=	pitch rate

## I. Introduction

**F**LYING aircraft in formation can lead to significant fuel savings due to the reduction in induced drag realized by the trailing

Presented as Paper 2012-4768 at the AIAA Conference on Guidance, Navigation, and Control, Minneapolis, MN, 13–16 August 2012; received 7 November 2012; revision received 26 April 2013; accepted for publication 30 April 2013; published online 31 January 2014. Copyright © 2013 by Maziar Hemati. Published by the American Institute of Aeronautics and Astronautics, Inc., with permission. Copies of this paper may be made for personal or internal use, on condition that the copier pay the \$10.00 per-copy fee to the Copyright Clearance Center, Inc., 222 Rosewood Drive, Danvers, MA 01923; include the code 1533-3884/14 and \$10.00 in correspondence with the CCC.

\*Ph.D. Candidate, Department of Mechanical and Aerospace Engineering; mhemati@ucla.edu. Member AIAA.

†Associate Professor, Department of Mechanical and Aerospace Engineering; eldredge@seas.ucla.edu. Senior Member AIAA.

‡Professor, Department of Mechanical and Aerospace Engineering; speyer@seas.ucla.edu. Fellow AIAA.

aircraft. This method of drag reduction is contingent upon having the trailing aircraft positioned properly within the upwash field of the lead aircraft's wake. The reduction in induced drag arising from flying aircraft in formation is, to first order, attributed to the rotation of the resultant force vector arising from the presence of the upwash field associated with the lead aircraft's wake [1,2]. As depicted in Fig. 1, the induced angle of attack due to the lead aircraft's upwash field leads to a decrease in induced drag (i.e.,  $\Delta D$  points in the direction of motion) and a small increase in lift. However, it has been shown by means of simplified linear analysis that 50% of the benefit is lost if the wake cannot be tracked within 10% span [1]. Based on this sensitivity to position within the wake, it is clear that accurate estimates of the wake location are essential for successful drag reduction in formation-flight missions.

Aircraft wake vortices and their contribution to induced drag comprise a broad body of technical literature and research. The review article by Spalart [3], and citations therein, summarize a tremendous amount of knowledge on aircraft trailing vortices, especially with regard to characterizing their formation, dynamics, and decay. Another review article by Kroo [4] summarizes fundamental aspects of induced drag and various drag-reduction concepts that take advantage of induced-drag physics. Additionally, an excellent overview of wake vortex research involving transport aircraft can be found in the article by Rossow [5].

The specific topic of formation-flying aerodynamics has been examined from a variety of standpoints. For example, some investigators have considered the optimal downwash and lift distribution of formation-flying wings [6], while others have focused on approaches for the modeling and simulation of aircraft formations [7,8]. Many groups have attempted to better characterize, by way of wind-tunnel measurements, the effect of tip vortices and wake roll-up on the trailing aircraft [9–13]. Numerous flight tests have also been conducted to determine real-world feasibility and proof-of-concept for formation-flying missions. Among these are the tests conducted at NASA Dryden Flight Research Center in 2001 on F/A-18 aircraft [2,14,15], as well as recent tests at Edwards Air Force Base in 2010 and 2012 on a formation of C-17 transport aircraft [16,17].

The issue of formation-flight control has also been the focus of several investigations. Giulietti et al. [18] have studied various aspects of formation-flight dynamics and control, while Campa et al. [19] have considered the design and flight testing of nonlinear formation control laws. There has also been much focus on real-time formation optimization by means of extremum-seeking control [20–23]. All of these studies consider formation aerodynamic effects as a function of the relative position between aircraft. This is a reasonable assumption for longitudinal separations on the order of a few wingspans but deteriorates as this separation increases. Due to safety restrictions, practical formation-flight missions will require

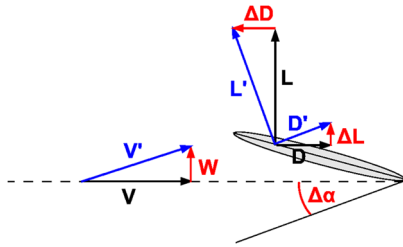


**Fig. 1** Rotation of resultant force on trailing aircraft due to lead aircraft's wake upwash. Drawn are the baseline forces, induced effects (prefixed with  $\Delta$ ), and formation forces (denoted with primes).

significant longitudinal separations. This poses a problem to approaches considered in these past studies, because the approaches are not robust to atmospheric turbulence and wind gusts that will most necessarily shift and modify wake characteristics in such a manner as to invalidate any wake estimates based on relative aircraft positions alone. Surely, constructing the aerodynamic benefit maps is more useful if they are referenced relative to the *wake* position directly.

The sensing and detection of wake vortices is not a new concept. Much research and technology development has focused on detecting wake hazards in the airspace and on airport runways. However, many such wake-detection tools require access to heavy, expensive, and complex instrumentation, such as radar, lidar, massive microphone and sodar arrays, and specialized acoustic transducer configurations [24–29]. Despite significant advances made for wake-hazard detection, these systems are primarily designed for ground use. The systems available for in-flight use, such as airborne lidar, remain impractical for operational use from both a cost and weight standpoint. More practical onboard sensor configurations, such as distributed pressure probes, have been applied to characterizing wake encounters as a postprocessing step [30–32]. Although these studies do not consider real-time algorithms for wake detection, they do demonstrate some practical instrumentation configurations that can be implemented for real-time wake sensing.

Other approaches for real-time vortex detection have also been considered in nonaircraft scenarios. For example, much work has been conducted on Lagrangian data assimilation for vortex detection in the atmospheric and oceanic sciences communities [33–35]. This work provides useful insight into general vortex detection but remains outside the scope of onboard wake sensing due to the need for Lagrangian measurements, which are unavailable for operational formation-flight missions. In 2003, Suzuki and Colonius [36] developed a method for detecting a vortex in a channel. This work is especially noteworthy due to its semblance to the approach taken in the present study, in that an array of pressure sensors is used to determine the vortex parameters of interest.

Despite all of the progress made in formation-flight research, it is clear that, to date, no reliable and practical methods for onboard wake estimation and sensing exist. Yet, knowledge of the wake location is essential to the success of formation-flight missions for drag reduction. As Blake and Multhopp [1] have shown, small deviations from the true wake location can lead to large losses in the drag benefit, thus indicating the absolute need for accurate and precise estimates of the wake position. The goal of wake sensing is to obtain reliable estimates of the wake location based on measurements taken from a suite of onboard sensors. The ultimate goal is to rely solely upon preexisting instrumentation; however, such a solution may not be physically possible.

By studying the wake-sensing problem in a simplified proof-of-concept setting, the present work attempts to identify and reconcile fundamental challenges associated with the general wake-estimation problem. The current development makes use of wing-distributed pressure sensors to extract the lead aircraft's wake parameters. Because the wake's upwash field is inherently distributed, the lead aircraft's wake leaves an aerodynamic signature across the trailing

aircraft's lifting surfaces. By assimilating measurements from wing-distributed sensors, the wake signature can be used to back out the wake location and other parameters of interest. The added advantage of such an approach is its ability to provide basic insights into the role of the fundamental wake nonlinearity associated with the upwash field. The wake-estimation algorithm developed here makes use of simple, but rich, aerodynamic models to reveal the fundamental aspects of the wake-sensing problem. In doing so, it is found that nonlinearities inherent to the wake's influence on the trailing aircraft can lead to undesirable behaviors under certain circumstances. In the present study it is shown that adopting more sophisticated nonlinear filtering paradigms and introducing aircraft dynamics can help mitigate some of these issues. The present work demonstrates that distributed aerodynamic measurements can be synthesized to successfully determine the wake parameters of a lead aircraft during formation flight in real time, at least in the simple configurations considered here.

The wake-estimation strategy is introduced and developed in Sec. II. Considerations of aerodynamic modeling and model integration with nonlinear estimation schemes are discussed. Section III presents the resulting performance of the wake-estimation strategy in a vortex lattice environment, followed by identification and reconciliation of the causes of estimation bias and filter divergence by means of empirical studies. Concluding remarks are made in Sec. IV.

## II. Estimator Design

In designing a reliable wake-estimation strategy, a representation of the wake's influence on the trailing aircraft must be considered. This representation will rely upon a model for the lead aircraft and its wake, as well as a model for the trailing aircraft's aerodynamic response due to the presence of this wake. The development of these models relies heavily on simple vortex entities such as vortex lines and horseshoes, which can be reviewed by the unfamiliar reader in Moran [37] and Katz and Plotkin [38]. Upon constructing a sufficiently realistic representation of the wake-aircraft interaction, standard Kalman-type and particle-filtering approaches from nonlinear filtering theory are invoked to define a suitable estimation algorithm.

The current section begins by introducing a model for the lead aircraft and its wake in Sec. II.A. Section II.B describes a lifting-line representation for the trailing aircraft in the presence of the lead aircraft's wake. With the aerodynamic modeling complete, the aerodynamic model is then integrated within the framework of various nonlinear estimation schemes in Sec. II.C. Kalman-type filters are considered, in addition to the particle filter. The various details of the wake-estimation algorithms are discussed in the ensuing subsections.

### A. Lead Aircraft and Wake Representation

The longitudinal separations experienced during formation-flight missions are large enough to allow the wake to roll up completely, thus making a horseshoe vortex model a reasonable representation of the lead aircraft and its wake. This can be further simplified by neglecting the influence of the bound vortex at large distances. In doing so, the semi-infinite horseshoe legs necessarily become infinite line vortices, with strength  $\Gamma_o$  and separation distance  $b$  dictated by the lead aircraft's weight and geometry, respectively. Because the trailing aircraft is not expected to undergo wake crossings during the wake identification segment of a formation-flight mission, a simple Biot–Savart relation can be used to express the velocity induced by each infinite line vortex at a point in space. Of course, a finite core size can be introduced to regularize vortices if deemed necessary, but this will not play a significant role in the estimator performance considered in the present development. The expression for the upwash field associated with the vortex wake can be obtained by linearly superposing the upwash field associated with each infinite line vortex individually:

$$w_o(y; \Gamma_o, y_o, z_o, b) = \frac{\Gamma_o(y - y_o + (b/2))}{2\pi[z_o^2 + (y - y_o + (b/2))^2]} - \frac{\Gamma_o(y - y_o - (b/2))}{2\pi[z_o^2 + (y - y_o - (b/2))^2]} \quad (1)$$

This nonlinear expression represents the wake's direct influence on the upwash field as a function of the wake parameters  $\Gamma_o$ ,  $y_o$ ,  $z_o$ , and  $b$ , as defined in Fig. 2. As will be seen, this nonlinear form is the fundamental nonlinearity associated with wake estimation.

### B. Trailing Aircraft Representation

With the lead aircraft's wake model established, it is now necessary to develop a mapping from the wake parameters to the trailing aircraft's aerodynamic response to it. The physics of the problem lends itself to a classical lifting-line approach, because formation-flying aircraft will likely only be subjected to slow time-scale (i.e., quasi-steady) maneuvers. The lifting-line model also has the advantage of being able to capture distributed aerodynamic quantities through only a small number of Fourier modes, thus keeping the dimensionality of the model small enough for real-time implementation. Here, the classical model is augmented with Eq. (1) to accommodate the presence of a nearby wake. Although more sophisticated modeling approaches can be considered to begin with, applying a lifting-line approach enables the effects of modeling error to be studied by simulating estimator performance in a more sophisticated setting (e.g., vortex lattice method).

Classical lifting-line theory represents the vorticity of the wing and its associated wake by a spanwise distribution of horseshoe vortices. The lifting-line integro-differential equations are then solved to determine the strength distribution along the lifting line. This strength distribution can then be used to compute other quantities of aerodynamic interest. The classical form of the lifting-line equation is [37]

$$\Gamma(y) = \frac{1}{2} U_\infty c(y) m_o(y) \left[ \alpha - \alpha_{l=0}(y) - \frac{1}{4\pi U_\infty} \oint_{-\tilde{b}/2}^{\tilde{b}/2} \frac{d\Gamma/d\eta}{y - \eta} d\eta \right] \quad (2)$$

with the boundary conditions

$$\Gamma(-\tilde{b}/2) = \Gamma(\tilde{b}/2) = 0 \quad (3)$$

Equations (2) and (3) are only valid for a wing in free space undergoing steady trimmed flight. If quasi-steady maneuvers in the presence of wake vortices are to be considered, as in Fig. 3, one must expand upon the expression just discussed by introducing additional terms to the upwash distribution along the wing's span. For example, any vertical translational velocity  $V_z$  will introduce a uniformly distributed downwash along the span. Additionally, rolling maneuvers (i.e., rotations about the body-fixed  $x$  axis) will induce a downwash proportional to the distance from the center of rotation  $\Omega_x y$ . Here, it is assumed that the center of rotation is located at midspan of the wing (i.e.,  $y_{C.G.} = 0$ ). Finally, pitching maneuvers (i.e., rotations about the body-fixed  $y$  axis) will introduce a

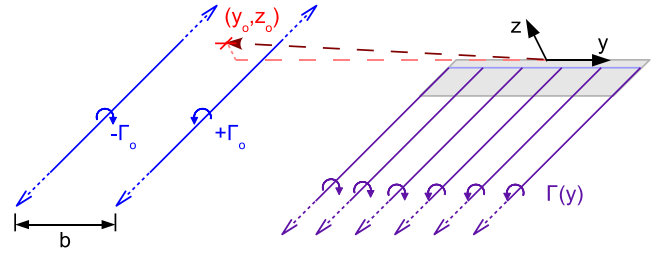


Fig. 3 The augmented lifting line model.

downwash proportional to the difference in position between the wing's center of gravity and the quarter-chord point  $\Omega_x(c_{1/4}(y) - x_{C.G.})$ . For the purpose of the present discussion, it will be assumed that  $c_{1/4} - x_{C.G.}$  is negligible, and thus, this term will be ignored. This assumption is also consistent with that of small sweep angles, which is inherent in the use of lifting-line theory in the first place. Finally, a term  $w_o(y; \Gamma_o, y_o, z_o)$  is included to represent the upwash distribution associated with the presence of a finite set of line vortices, thus accounting for the presence of the wake.

The final form of this generalized lifting-line integro-differential equation becomes

$$\Gamma(y) = K_L(y) \left[ U_\infty [\alpha(y) - \alpha_{l=0}(y)] - V_z - \Omega_x y + w_o(y; \Gamma_o, y_o, z_o) - \frac{1}{4\pi} \oint_{-\tilde{b}/2}^{\tilde{b}/2} \frac{d\Gamma/d\eta}{y - \eta} d\eta \right] \quad (4)$$

where  $K_L(y) := (1/2)c(y)m_o(y)$ , with the boundary conditions

$$\Gamma(-\tilde{b}/2) = \Gamma(\tilde{b}/2) = 0 \quad (5)$$

In the approach taken here, this set of equations is solved by the collocation method [37]. Once this integro-differential equation is solved for the  $\Gamma(y)$  distribution, many other terms of interest easily follow. For example, it can be shown that for a flat plate, the distribution of differential pressure coefficient will take the form

$$\Delta C_p(x, y) = -4 \frac{\Gamma(y)}{\pi U_\infty c(y)} \left( \frac{c(y)}{x} - 1 \right)^{1/2} \quad (6)$$

### C. Wake-Estimation Algorithm

Having developed the necessary aerodynamic models, a viable estimation strategy based on various nonlinear estimation approaches can be developed. First, Kalman-type algorithms will be considered due to their computational simplicity and ability to handle process and measurement uncertainty. Particle filters are also used to better handle the nonlinearities associated with the wake. All of the wake estimators developed in this work follow the same underlying approach (i.e., synthesizing distributed aerodynamic measurements with the aid of the augmented lifting-line model), but do so by means of different nonlinear stochastic estimation algorithms.

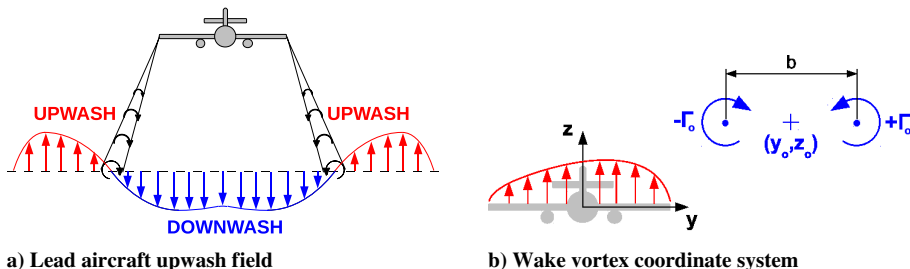


Fig. 2 Schematic representation of the lead aircraft's wake and its aerodynamic influence on the trailing aircraft.

Each of the following sections highlights an important aspect of the overall wake-estimation strategy. The discussion begins by defining the state and measurement vectors in Sec. II.C.1, followed by a discussion of the associated measurement and process noise in Sec. II.C.2. Some necessary details related to Kalman-type and particle filters are presented in Secs. II.C.3 and II.C.4, respectively. Regardless of the specific algorithm employed, an out-of-formation calibration must be performed before operating the wake estimator. Discussion of this process is presented in Sec. II.C.5. Finally, the specific aircraft dynamics considered in this study are described in Sec. II.C.6.

### 1. States and Measurements

For the current discussion, the following definitions are used for the states  $\mathbf{x}$  and measurements  $\mathbf{z}$ :

$$\mathbf{x} := \begin{bmatrix} \Gamma_o \\ y_o \\ z_o \end{bmatrix} \in \mathbb{R}^3 \quad \text{and} \quad \mathbf{z} := \begin{bmatrix} \Delta C_{p_1} \\ \vdots \\ \Delta C_{p_i} \\ \vdots \\ \Delta C_{p_M} \end{bmatrix} \in \mathbb{R}^M \quad (7)$$

Here, the states to be estimated are those associated with the relevant vortex parameters (see Figs. 2 and 3): 1) the strength of the pair  $\Gamma_o$ , and 2) the lateral and vertical positions of the wake origin (i.e., the center of the vortex pair) relative to the aircraft's body-fixed coordinate system  $(y_o, z_o)$ .

Though estimating the relative position of the wake is the central concern, the associated vortex strength is an additional, but necessary, parameter to be estimated. Previous studies showed degraded estimator performance without the inclusion of this additional parameter. This will be discussed further in Sec. III.A. Future investigations may also consider other wake parameters, such as relative roll and relative yaw angles.

In the current implementation, spanwise differential pressure distribution is used as a measurement. The reason for this choice lies in simplifying the estimator's development process. Because the  $\Gamma(y)$  distribution solved for within the lifting-line model is directly related to  $\Delta C_p(y)$  via Eq. (6), the differential pressure distribution has been chosen as the measurement within the current framework. Other measurements, such as angle of attack distribution, may also have merit. More importantly, the current algorithms are not restricted to distributed measurements alone; however, the use of distributed measurements allows valuable insights to be gained, so it is useful to consider such approaches first. If estimators relying upon distributed measurements lack in performance, then relying upon integrals over these distributions will be even more lacking. Although the ultimate hope is to rely upon existing onboard instrumentation exclusively for measurement data, validation under the distributed measurement framework must come first.

### 2. Measurement and Process Noise

The wake estimator to be designed is desired to be robust to both measurement and process noise. As a result, such effects must be accounted for within the estimation procedure. The Kalman-type and particle-filtering algorithms already take such effects into account. In the present development, the process noise is currently only accounted for through the process covariance matrix  $W_k \in \mathbb{R}^{3 \times 3}$ . No additive process noise is explicitly added within the system model. Instead, process noise is implicitly introduced by means of model mismatch between the estimator model and the simulation environment. In an effort to keep the filter open, enforcement of  $W_k > 0$  is ensured. Because there is no process noise explicitly introduced within the simulation framework,  $W_k$  can be considered as a tuning parameter to be used in conditioning the filter for better performance.

Unlike the process noise, the measurement noise is explicitly introduced within the simulation. That is, the inputted measurement is assumed to have a white-noise signal  $\mathbf{v}_k \sim \mathcal{N}(0, V_k)$  added to it.

Here, it is assumed that the measurement has a "true" covariance of  $V_k^{\text{true}} \in \mathbb{R}^{M \times M}$  when introducing noise to the measurement; however, within the filtering framework,  $V_k$  is treated as a tuning parameter. As such,  $V_k$  as defined within the context of the filter is not necessarily equal to  $V_k^{\text{true}}$ , and can be used to tune the filter.

Finally, the initial estimate for the vortex parameters is assumed to be  $\hat{\mathbf{x}}_o \sim \mathcal{N}(\bar{\mathbf{x}}_o, M_o)$ . Again, the true estimate may have an initial covariance  $M_o^{\text{true}} \in \mathbb{R}^{3 \times 3}$ , but  $M_o$  is treated only as a tuning parameter within the context of the filter. That is, process noise is not explicitly introduced within the simulations (i.e.,  $M_o^{\text{true}} = 0$ ); rather, it is assumed that any modeling error can be accounted for with a suitable choice of  $M_o$  in the filter initialization.

### 3. Kalman-Type Filtering: Measurement Function Linearization

Kalman-type filters are one class of nonlinear estimation algorithm in this study. In the interest of brevity, familiarity with Kalman-type filtering is assumed. The reader is referred to Jazwinski [39] and Speyer and Chung [40] for further details regarding such algorithms. The present section only discusses computation of the measurement Jacobian matrix  $H$ , which is required by Kalman-type filtering algorithms. For the vortex parameters  $\mathbf{x}$  just given, this takes the form

$$H = \begin{bmatrix} \frac{\partial \Delta C_{p_1}}{\partial \Gamma_o} & \frac{\partial \Delta C_{p_1}}{\partial y_o} & \frac{\partial \Delta C_{p_1}}{\partial z_o} \\ \vdots & \vdots & \vdots \\ \frac{\partial \Delta C_{p_i}}{\partial \Gamma_o} & \frac{\partial \Delta C_{p_i}}{\partial y_o} & \frac{\partial \Delta C_{p_i}}{\partial z_o} \\ \vdots & \vdots & \vdots \\ \frac{\partial \Delta C_{p_M}}{\partial \Gamma_o} & \frac{\partial \Delta C_{p_M}}{\partial y_o} & \frac{\partial \Delta C_{p_M}}{\partial z_o} \end{bmatrix} \in \mathbb{R}^{M \times 3} \quad (8)$$

In the current implementation, the measurement Jacobian is computed numerically via first-order finite differences applied to small perturbations about the nominal (estimated) state. This approach simplifies future modifications to the filter model. For example, if new measurements (i.e., not differential pressures) are desired, the function  $\mathbf{h}_k(\mathbf{x}_k)$  is the only portion of the filter that will require modification.

### 4. Particle-Filtering Procedure

The second class of nonlinear estimation algorithm considered in this study is the particle filter (PF). PFs approximate the Bayesian optimal filtering equations by means of Monte Carlo methods. The a posteriori probability density is represented by a set of random samples, or "particles," with associated weights. As the number of particles increases, the representation approaches the exact functional description of the probability distribution [41].

As time progresses, the PF algorithm can lead to degeneracy due to overweighting a few samples, leaving the remaining ones useless. A common method of circumventing this issue comes in the form of a "resampling" step. The sequential important resampling PF algorithm implemented in the present study makes use of a simple cumulative sum algorithm to resample particles at every time step. Further details regarding particle filters and resampling algorithms can be found in Ristic et al. [41].

### 5. Offline Calibration

Thus far, all of the algorithmic details for the wake estimator have been established. The important step of ensuring that the model implemented within the estimator matches up reasonably well with reality still needs to be addressed. Thus, before "hooking up" the filter, the lifting-line model within the filter needs to be calibrated in an isolated flight configuration. That is, the lifting-line model must be calibrated against the actual measurement data offline to initialize the model for best performance. This is done by determining a linear gain vector ( $\mathbf{k}_{\text{cal}} \in \mathbb{R}^M$ ) to apply to the model output:

$$\mathbf{k}_{\text{cal}} := [k_{\text{cal},1} \ \cdots \ k_{\text{cal},i} \ \cdots \ k_{\text{cal},M}]^T, \quad (9)$$

$$\text{where } k_{\text{cal},i} := \frac{z_{i,\text{Measured}}}{z_{i,\text{LiftingLine}}}$$

Calibration is important in the case of both simulation and flight testing. Within the context of simulation, calibration allows the filter to better account for variations between aerodynamic models used to represent truth. For example, aerodynamic effects from the fuselage and other blunt bodies, unaccounted for by the lifting-line model, can be accommodated. Such calibration is also necessary for actual flight implementation because, in addition to modeling inaccuracies, unaccounted sensor biases may be present. In the case of pressure transducers, for example, such biases can be caused from installation or manufacturing errors. Calibrating the system offline introduces an element of robustness to the model, because sensor biases can be better accounted for.

### 6. System Dynamics

The relative aircraft motions between two formation-flying aircraft, considered in the present study, are described in the present section. The system dynamics studied in the current effort are simply prescribed sinusoidal changes in the relative vertical and lateral displacements between the wing and wake axes. Moreover, the constant amplitude and frequency of the sinusoidal velocity by which the wing moves is assumed to be fully known (i.e., there is no variance associated with these parameters). The vertical velocity of the wing influences the induced drag and, therefore, the pressure measurements. This is accounted for within the lifting-line implementation. The lateral velocity is prescribed only for the purpose of “increasing the observability” of the vortex pair. Such prescribed motions are expected to increase the observability of the vortex pair because, though  $\mathbf{h}_k(\mathbf{x}_k)$  is not necessarily invertible for all values of  $\mathbf{x}_k$ , the prescribed motions are more likely to describe a set  $[\mathbf{h}_1(\mathbf{x}_1), \dots, \mathbf{h}_{k-1}(\mathbf{x}_{k-1}), \mathbf{h}_k(\mathbf{x}_k)]$  that can only be generated from a unique set of vortex parameters.

The lateral and vertical velocity components of the wing are denoted as  $V_y(t_k)$  and  $V_z(t_k)$ , respectively. For the purpose of simulation, the wake is moved with respect to the aircraft rather than the aircraft moved with respect to the wake. In doing so, upwash/sidewash effects due to motions of the lifting surfaces can be ignored. This provides a greater opportunity for distinguishing the wake’s upwash signature, because it is less likely to be “washed out” by the presence of these additional disturbance fields. Thus, for purposes of the estimator simulation, one may consider that the wing “sees” the vortex pair move with equal but opposite velocity components, ignoring all velocities due to motion of the solid bodies. Hence

$$y_o^{(k+1)} = y_o^{(k)} - V_y(t_k)\Delta t_k \quad (10)$$

$$z_o^{(k+1)} = z_o^{(k)} - V_z(t_k)\Delta t_k \quad (11)$$

where  $\Delta t_k$  is the time period between sensor measurements. In other words, the dynamical equations for this system can be written as

$$\begin{bmatrix} \Gamma_o \\ y_o \\ z_o \end{bmatrix}_{k+1} = \begin{bmatrix} \Gamma_o \\ y_o \\ z_o \end{bmatrix}_k + \begin{bmatrix} 0 \\ -V_y(t_k)\Delta t_k \\ -V_z(t_k)\Delta t_k \end{bmatrix} \quad (12)$$

Although other aspects of the aircraft dynamics have not been included here (e.g., roll and yaw kinematics), they will be considered in future works. In the present study, only fundamental aspects of the filter have been considered. As such, only parameters that are expected to demonstrate the capabilities of the filter have been included. Keeping the number of parameters to a minimum also allows the study to be kept as intuitive as possible.

## III. Performance Results

As previously mentioned, the classical lifting-line approach used in designing the estimator can be replaced with more sophisticated aerodynamic models (e.g., modern/extended lifting-line methods or vortex lattice methods) in the future. However, the classical lifting-line method was selected primarily due to its simplicity. Because the current focus is on the assessment of an estimation algorithm, the aerodynamic model must only be capable of capturing the class of nonlinearity associated with the process. Classical lifting-line theory is entirely capable of doing this; it also provides a simple framework for tracking the influence of the fundamental wake nonlinearity on the overall estimator dynamics. Additionally, by considering a simple model at this time, the effects of modeling error can be studied directly by simulating estimator performance in a more sophisticated environment. Here, vortex lattice simulations of a generic aircraft equipped with five wing-distributed pressure sensors ( $M = 5$ ) have been studied to assess the wake-estimation algorithm’s performance characteristics. The simplest possible aircraft is chosen for the present study because of the limitations associated with the classical lifting-line approach in modeling sophisticated geometries such as sweep and dihedral. Despite these limitations, the calibration procedure described in Sec. II.C.5 is able to reduce the estimator’s sensitivity to the presence of unmodeled features, such as horizontal and vertical stabilizers.

Two main types of simulations are considered in the vortex lattice results that follow: 1) static configuration, in which there is no relative motion between the aircraft and wake, and 2) prescribed relative motions, in which relative kinematics are prescribed between the aircraft and wake a priori, thus introducing “dynamics.”

In both of these instances, the same aircraft/sensor configuration is used (see Fig. 4). The level of noise associated with the sensor measurements is also consistent in both cases. Process noise is not present in the simulation, though a finite “truth” process noise is assumed for use in tuning the estimator. The corresponding noise levels are

$$\sigma_v^{\text{true}} = 1 \times 10^{-5}, \quad \sigma_w^{\text{true}} = 1 \times 10^{-3}$$

where  $\sigma_w^{\text{true}}$  refers to the initial uncertainty in the estimate (i.e.,  $M_o$  discussed in Sec. II.C.2) and is currently treated as a tuning parameter. Unless otherwise stated, the remaining estimator tuning parameters have the following values:

$$\sigma_v = 7 \times 10^{-3}, \quad \sigma_w = 3 \times 10^{-2}$$

Finally, all values are presented in dimensionless form, using wing span, flight speed, and air density at 28,000 ft as factors for non-

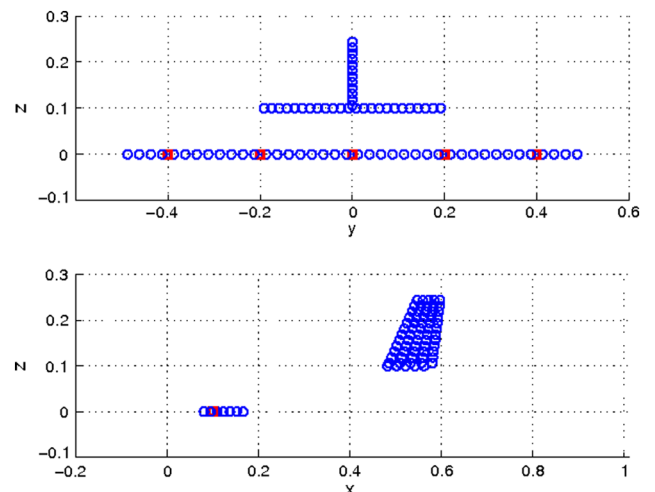


Fig. 4 Vortex lattice simulation aircraft configuration. Collocation points are denoted by  $\circ$ , while pressure sensors are denoted by  $\square$ .

**Table 1 Specifications of the cases studied based on case number, wake parameters, kinematics, and filtering algorithm**

Case number	Wake parameters ( $\Gamma_o, y_o, z_o$ )	Kinematics	Filtering algorithm
1	(0.03, -1, 0)	Static <sup>a</sup>	Extended Kalman filter
2a	(0.03, -1.5, 1)	Static	Extended Kalman filter
2b	(0.03, -1.5, 1)	Static	Particle filter
3	(0.03, -1, 0)	$A = 0.05, \omega = 0.05$	Extended Kalman filter
4a	(0.03, -1.5, 1)	$A = 0.5, \omega = 0.05$	Extended Kalman filter
4b	(0.03, -1.5, 1)	$A = 0.5, \omega = 0.001$	Extended Kalman filter

<sup>a</sup>“Static” refers to a configuration with no relative motions between aircraft and wake, while cases with relative motions are defined with respect to the kinematic parameters  $A$  and  $\omega$  defined in Sec. III.B.

dimensionalization. A list of the various cases studied is presented in Table 1.

### A. Two-Aircraft Static Configuration

Several simulation results for the case of no relative motions are now presented. Case 1, presented in Fig. 5, provides a validation for a simple case using an extended Kalman filter (EKF); the wake is close to the trailing aircraft, thus leaving a relatively strong signature on it. Based on both the estimation trajectory map and the error histories, one can see that the estimator does a reasonable job zeroing in on the

relative wake location. The estimate of the wake strength, however, does not perform as well. The error associated with the estimate of  $\Gamma_o$  is on the same order of the quantity itself. An interesting point to note is that this tends to be a common trend among most of the simulations conducted. Several studies were previously conducted, albeit briefly, on the effect of removing the wake strength  $\Gamma_o$  as a parameter to be estimated (i.e., assuming  $\Gamma_o$  is fully known). Surprisingly, the results of these simulations led to degraded estimator performance! This can be explained by reflecting on the large amount of error present in  $\Gamma_o$  when it is included as an estimation parameter. It

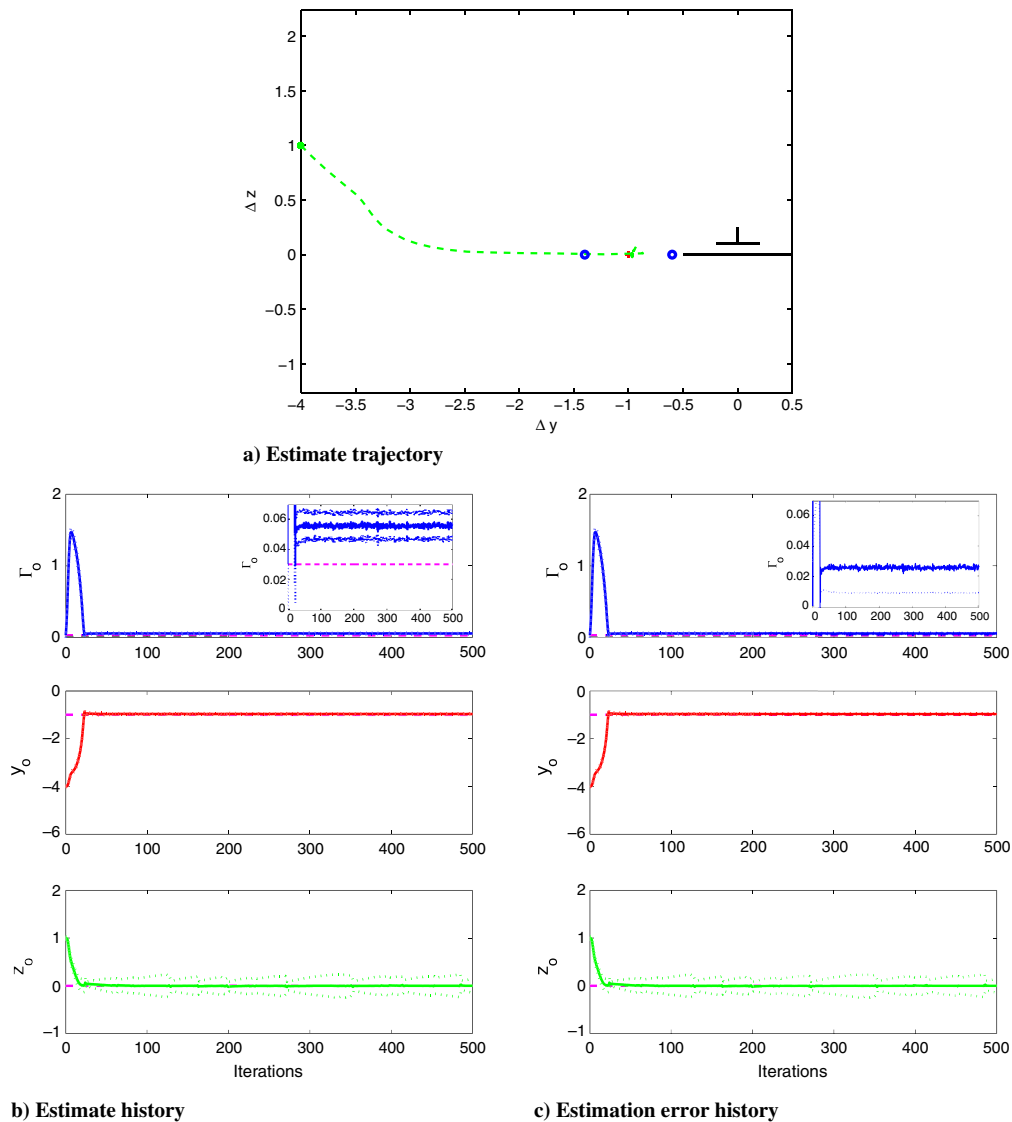


**Fig. 5 Case 1 simulation results.** In a),  $\circ$  denotes the wake vortex core and  $+$  the wake center, the trailing (estimating) aircraft is drawn flying into the page, with initial estimate  $\bullet$  and estimation trajectory  $---$ . In b) and c), solid lines denote estimates, dotted lines are 1- $\sigma$  bounds, and dashed lines are true values.

turns out that much of the process uncertainty is lumped into  $\Gamma_o$ . As a result, when it is removed as an estimation parameter, the estimates of the wake coordinates are more greatly affected by these uncertainties. Because the wake coordinates are the parameters of interest in formation-flight applications, the poor estimate of  $\Gamma_o$  is not of great concern and is kept so as to improve the quality of  $(y_o, z_o)$  estimates.

Case 2 considers a configuration with one and one-half wing spans of lateral separation and one wing span of vertical separation. Two different classes of nonlinear estimation algorithms were considered in this study: 1) Kalman-type filters, and 2) particle filters. The Kalman-type filters consisted of an EKF (case 2a), an iterated Kalman filter, and a second-order Kalman filter. These three Kalman-type filters yielded similar results (only EKF results are presented in the interest of brevity), all of which led to significant biases or filter divergence depending on the initial estimates. Based on the resulting bias and divergence from these studies, a particle filter (case 2b) was also implemented in an effort to empirically determine the cause of the bias and/or divergence. A particle filter is capable of passing statistics through the wake nonlinearity directly, not relying on linearizations as the Kalman-type filters do. This enables a study of the effects of the nonlinear structure on estimator performance. Based

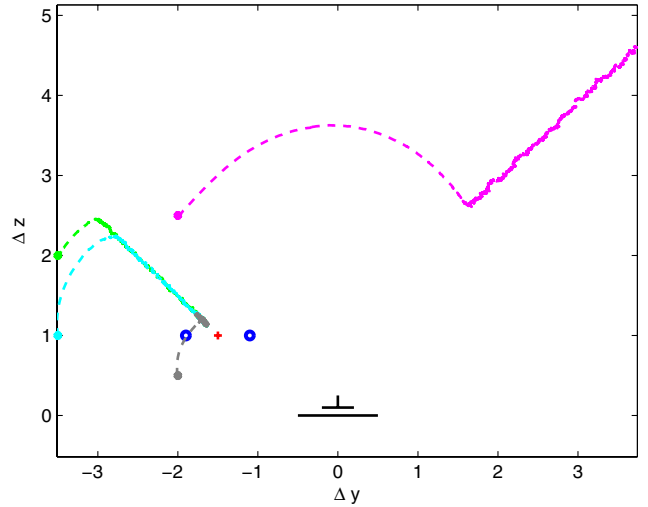
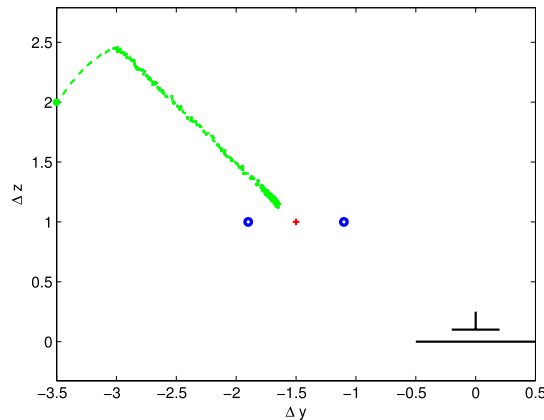
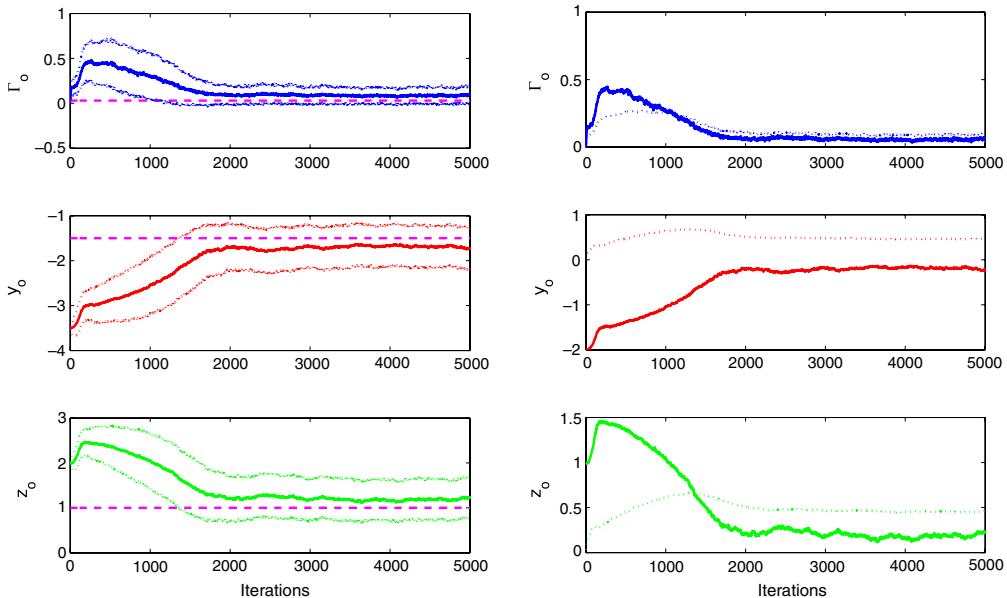


Fig. 7 Case 2a results from multiple initial estimates, where  $\circ$  denotes a wake vortex core and  $+$  the wake center, the trailing (estimating) aircraft is drawn flying into the page, with initial estimates  $\bullet$  and estimation trajectories  $—$ .



a) Estimate trajectory



b) Estimate history

c) Estimation error history

Fig. 6 Case 2a simulation results. In a),  $\circ$  denotes the wake vortex core and  $+$  the wake center, the trailing (estimating) aircraft is drawn flying into the page, with initial estimate  $\bullet$  and estimation trajectory  $—$ . In b) and c), solid lines denote estimates, dotted lines are  $1-\sigma$  bounds, and dashed lines are true values.

on the vortex lattice simulations, the particle filter alleviated the bias issues, but divergence was still a problem. This indicates a potential unobservability that is not being handled properly by the sensor configuration. Introducing relative motions between aircraft will be shown to mitigate this divergence issue by modifying the observability structure of the wake.

### 1. Extended Kalman Filter

The EKF in Case 2a, presented in Figs. 6 and 7, reveals the presence of attractors in the estimation error space. The position estimate follows a similar trajectory for several different initial estimates and always leads to the same biased position estimate. In one of the cases presented, the estimate actually diverges! The wake nonlinearity and its associated observability structure are responsible for this behavior. Methods for handling this nonlinear and unobservable structure are presented in the ensuing sections.

### 2. Particle Filter

The wake nonlinearity is a likely culprit leading to the biases in some of the estimation results. By invoking a PF (case 2b), the nonlinearity can be handled directly; if the PF gets rid of the bias and divergence issues, it can be safely stated that the nonlinear structure of

the wake requires direct processing (i.e., linearizations are not sufficient) to achieve favorable estimator performance. In implementing the PF for wake estimation, the following parameter values are used:

$$N_p = 1000, \quad \sigma_v = 3 \times 10^{-4}, \quad \sigma_w = 1 \times 10^{-2}$$

The PF results, presented in Figs. 8 and 9, demonstrate the greatest performance among the four wake-estimation algorithms studied. Because the PF propagates statistics through the vortex nonlinearity directly, without relying upon successive linearizations, the biases due to small modeling errors are minimized. However, as a result of system unobservability, the estimates continue to diverge along the magenta path. In other words, the biases observed in the Kalman-type filters were caused due to the strong nonlinearity associated with the wake's influence, but the divergence is likely rooted in the observability structure of the wake.

### B. Two Aircraft with Relative Motions

The divergence issues arising in cases 2a and 2b are most likely attributed to wake unobservability. Because the PF also exhibited the same divergent behavior, the wake nonlinearity cannot be blamed for

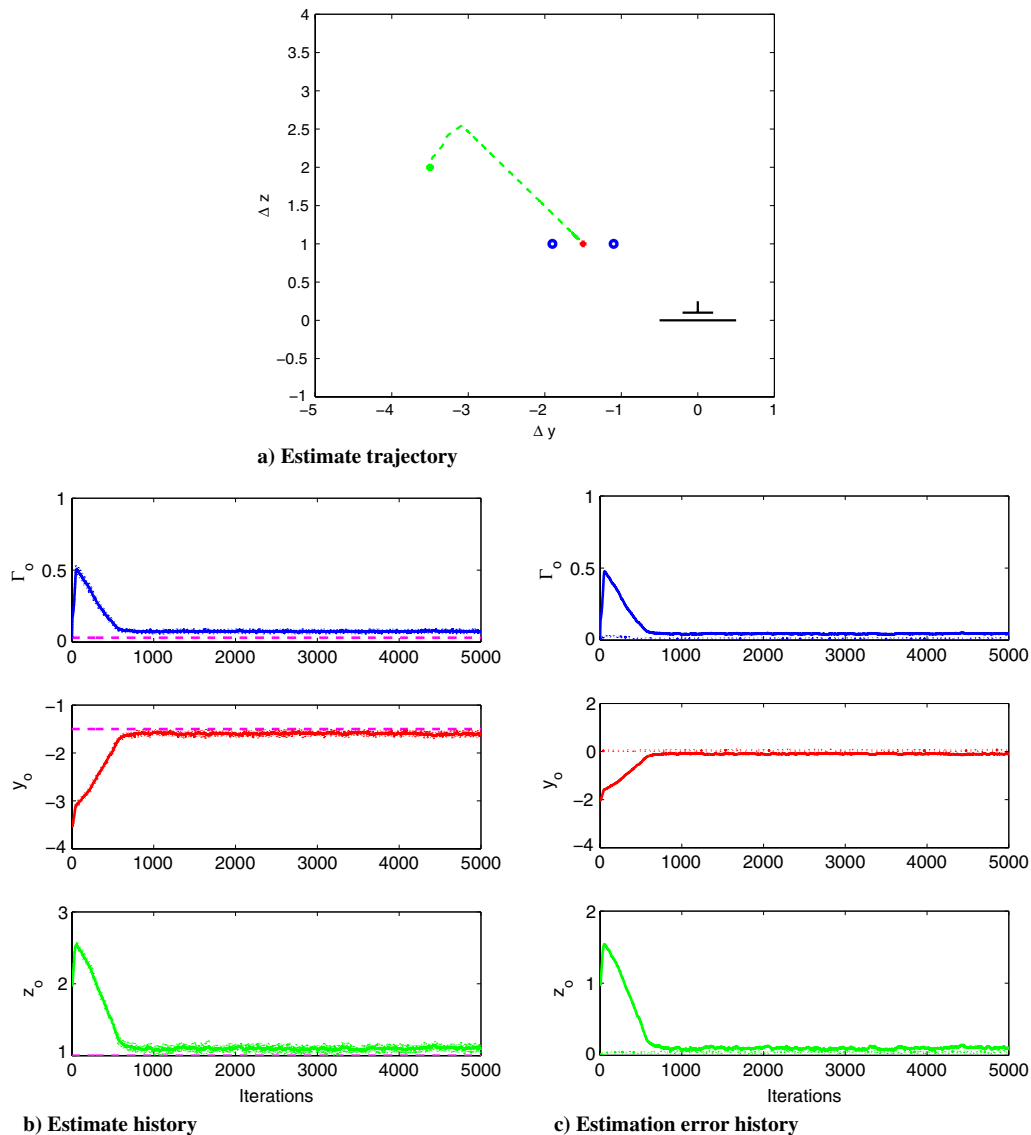


**Fig. 8** Case 2b simulation results. In a),  $\circ$  denotes the wake vortex core and  $+$  the wake center, the trailing (estimating) aircraft is drawn flying into the page, with initial estimate  $\bullet$  and estimation trajectory  $—$ . In b) and c), solid lines denote estimates, dotted lines are  $1-\sigma$  bounds, and dashed lines are true values.

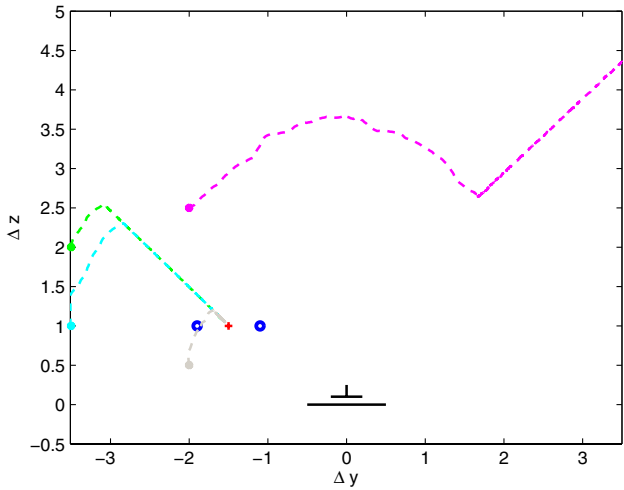


Fig. 9 Case 2b results from multiple initial estimates, where  $\circ$  denotes a wake vortex core and  $+$  the wake center, the trailing (estimating) aircraft is drawn flying into the page, with initial estimates  $\bullet$  and estimation trajectories  $— —$ .

this shortcoming. To empirically verify that the observability structure of the wake is responsible for divergence, the following section considers the effect of relative motion on the performance of the wake-estimation algorithm. It is hypothesized that introducing relative motions between the aircraft and the wake can lead to improvements in the wake’s observability structure, which should aid in resolving filter divergence. As the aircraft moves closer to the wake, the signature becomes more pronounced. Thus, a time sequence of wake signatures should be more revealing than a single wake signature with additive noise.

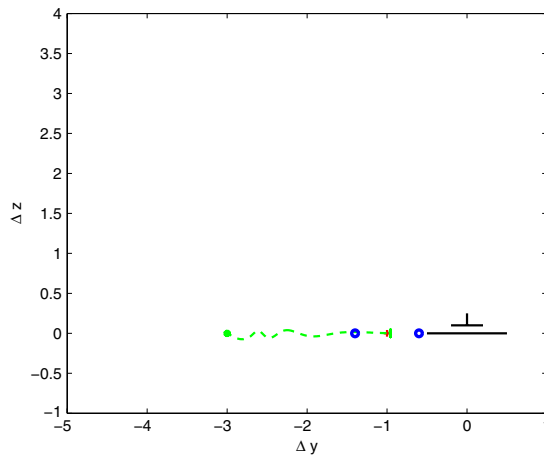
In the present study, only lateral dither signals are introduced. These relative lateral motions are prescribed as

$$\mathbf{x}_{k+1} = F_k \mathbf{x}_k + \Lambda_k \mathbf{u}_k$$

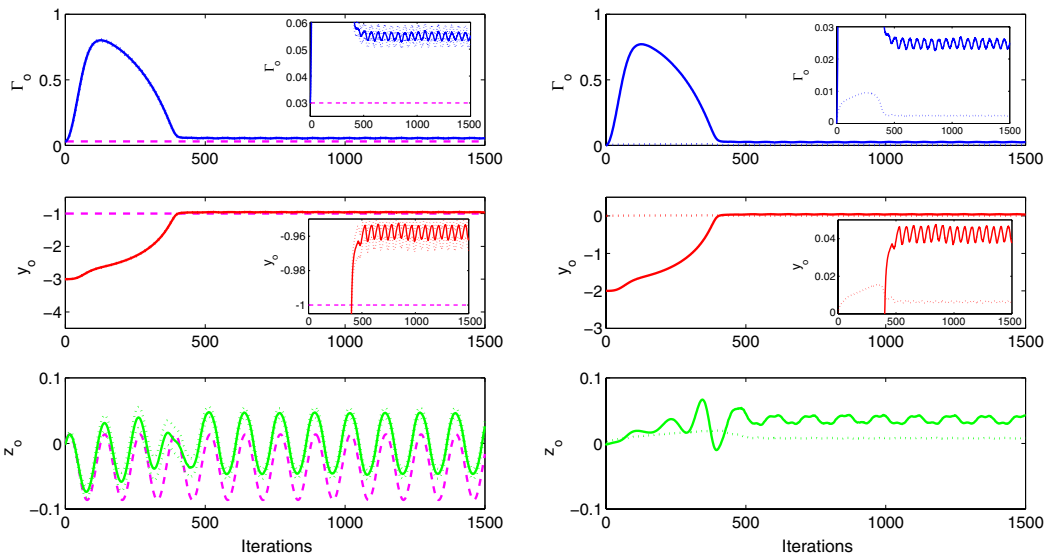
where

$$F_k = I^{N \times N} \quad \Lambda_k = \begin{bmatrix} 0 & 0 \\ A\omega & 0 \\ 0 & 0 \end{bmatrix} \quad \mathbf{u}_k = \begin{bmatrix} \cos(\omega t) \\ 0 \end{bmatrix}$$

with time quantities normalized by  $\Delta t$ , the time period between subsequent sensor measurements. Because these tests address the



a) Estimate trajectory



b) Estimate history

c) Estimation error history

Fig. 10 Case 3 simulation results. Note  $\sigma_w = 1 \times 10^{-3}$  for this case only. In a),  $\circ$  denotes a wake vortex core and  $+$  the wake center, the trailing (estimating) aircraft is drawn flying into the page, with initial estimate  $\bullet$  and estimation trajectory  $— —$ . In b) and c), solid lines denote estimates, dotted lines are  $1-\sigma$  bounds, and dashed lines are true values.

observability structure of the wake, only the EKF results with various values of  $A$  and  $\omega$  are presented here.

A simple example of the incorporation of kinematics is presented via case 3 in Fig. 10. Although the estimate appears to lock in on the  $z_o$  value in terms of phase, the actual estimate has a periodic error value in steady state. Though not apparent under such weak forcing magnitude, the unforced channels (i.e.,  $\Gamma_o$  and  $z_o$ ) also have periodic values appearing in steady state.

Cases 4a and 4b consider different sets of lateral dither parameters, leading to significantly different performance characteristics. It is found that the divergent behavior of the estimator in cases 2a and 2b (c.f. Fig. 7) can be eliminated under the kinematics prescribed in case 4a (c.f. Fig. 11). However, the resulting converged estimate is far from the correct value. On the other hand, the kinematics prescribed in case 4b (c.f. Fig. 12) continues to result in filter divergence, thus demonstrating that prescribing kinematics does not guarantee convergence. This clearly demonstrates that arbitrary motions alone are not sufficient to yield performance gains. Although dynamics have been shown to influence the wake's observability structure, further study is needed in this area. The influence of dynamics on optimal system observability and estimator performance must be carefully studied if vortex-based wake estimation is to be successful in practice.

Additional factors to be considered in the optimal observability problem include sensor array configurations and additional classes of

sensors. Such studies may require substitution of the lifting-line model with more sophisticated models, such as extended lifting-line or vortex lattice models, to handle additional geometric complexities and multibody sensor distributions. These methods are analogous to classical lifting-line methods and operate on the wake nonlinearity in a similar manner to attain aerodynamic quantities of interest. Though the computational demand of these methods is greater than that of the classical lifting-line method, several strategies exist for keeping the cost at a level amenable to real-time implementation. For example, the collocation matrices associated with lattice methods can be precomputed, assuming the aircraft geometry itself does not undergo significant changes. Additional approaches may rely upon table look-ups for distributed aerodynamic quantities based on the set of vortex parameters; however, such methods tend to suffer from large memory burdens associated with storing the aerodynamic tables.

With a better handle of wake observability by means of these proposed studies, it may be possible to use integrated values of the aerodynamic quantities to say something about the wake parameters reliably as well. For example, by integrating the pressure distribution, the forces and moments can be deduced. Because this is a linear operation of the pressures, it remains a linear mapping of the wake nonlinearity. The necessary conditions for successful wake sensing will still include the conclusions made in the present study. However, by relying upon forces and moments, much of the signature associated with the wake is lost, and greater complexity is introduced

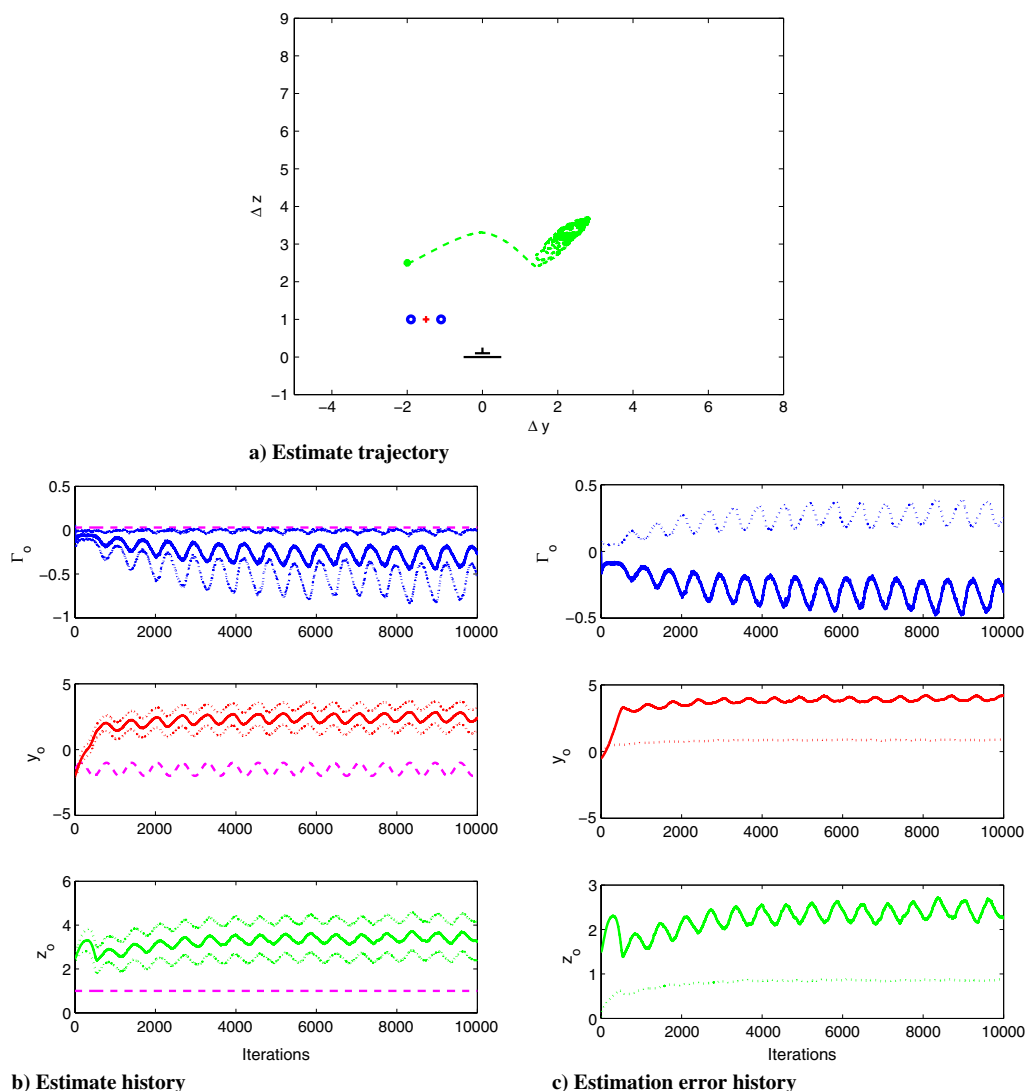


**Fig. 11** Case 4a simulation results. In a),  $\circ$  denotes a wake vortex core and  $+$  the wake center, the trailing (estimating) aircraft is drawn flying into the page, with initial estimate  $\bullet$  and estimation trajectory  $---$ . In b) and c), solid lines denote estimates, dotted lines are  $1-\sigma$  bounds, and dashed lines are true values.

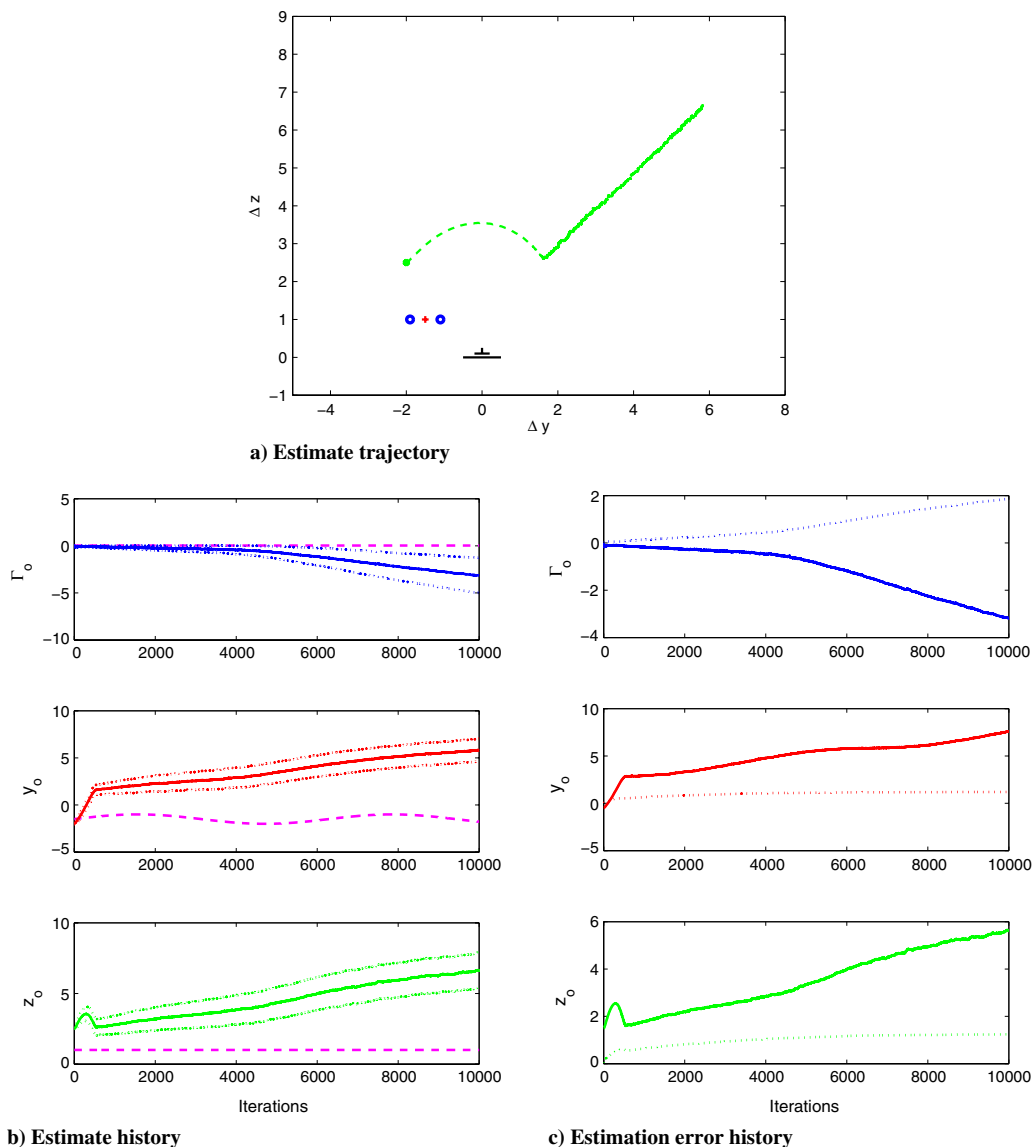


**Fig. 12** Case 4b simulation results. In a),  $\circ$  denotes a wake vortex core and  $+$  the wake center, the trailing (estimating) aircraft is drawn flying into the page, with initial estimate  $\bullet$  and estimation trajectory  $---$ . In b) and c), solid lines denote estimates, dotted lines are  $1-\sigma$  bounds, and dashed lines are true values.

to the problem by reducing the fidelity of the measurements to be incorporated. As a result, such an approach will require further studies of observability optimization. The ultimate wake-estimation algorithm will likely make use of both force and moment measurements as well as distributed aerodynamic quantities to make reliable estimates of the wake location.

#### IV. Conclusions

By focusing on simple wake and trailing aircraft representations, the current study has made much progress in understanding the nature of wake estimation and in demonstrating a viable wake-sensing strategy based on distributed aerodynamic measurements. Multiple attractors have been identified in the estimation error space associated with Kalman-type filters acting on the wake nonlinearity. Particle filters have been shown to alleviate this resulting bias, though divergence issues associated with the wake observability structure still remain an issue in static formations. Wake observability can be improved through relative motions between the aircraft and the wake, which helps alleviate the divergence issues encountered in static formation. Further study of the effect of relative motions on the observability structure of the wake and on the performance of the wake estimators is a necessary endeavor.

#### References

- [1] Blake, W., and Multhopp, D., "Design, Performance and Modeling Considerations for Close Formation Flight," AIAA Paper 1998-4343, Aug. 1998.
- [2] Ray, R. J., Cobleigh, B. R., Vachon, M. J., and St. John, C., "Flight Test Techniques Used to Evaluate Performance Benefits During Formation Flight," NASA TP-2002-210730, Aug. 2002.
- [3] Spalart, P. R., "Airplane Trailing Vortices," *Annual Review of Fluid Mechanics*, Vol. 30, Jan. 1998, pp. 107–138. doi:10.1146/annurev.fluid.30.1.107
- [4] Kroo, I., "Drag Due to Lift: Concepts for Prediction and Reduction," *Annual Review of Fluid Mechanics*, Vol. 33, Jan. 2001, pp. 587–617. doi:10.1146/annurev.fluid.33.1.587
- [5] Rossow, V. J., "Lift-Generated Vortex Wakes of Subsonic Transport Aircraft," *Progress in Aerospace Sciences*, Vol. 35, No. 6, 1999, pp. 507–660. doi:10.1016/S0376-0421(99)00006-8
- [6] Frazier, J. W., and Gopalathnam, A., "Optimum Downwash Behind Wings in Formation Flight," *Journal of Aircraft*, Vol. 40, No. 4, 2003, pp. 799–803. doi:10.2514/2.3162
- [7] Marino, L., "A Simple Model Revisited for Wing–Wings and Wings–Ground Interference Problems," AIAA Paper 2003-4063, June 2003.
- [8] Wang, Z., and Mook, D. T., "Numerical Aerodynamic Analysis of Formation Flight," AIAA Paper 2003-610, Jan. 2003.

- [9] Bangash, Z. A., Sanchez, R. P., Ahmed, A., and Khan, M. J., "Aerodynamics of Formation Flight," *Journal of Aircraft*, Vol. 43, No. 4, 2006, pp. 907–912.  
doi:10.2514/1.13872
- [10] Bramesfeld, G., and Maughmer, M. D., "Effects of Wake Rollup on Formation-Flight Aerodynamics," *Journal of Aircraft*, Vol. 45, No. 4, 2008, pp. 1167–1173.  
doi:10.2514/1.33821
- [11] Gingras, D. R., "Experimental Investigation of a Multi-Aircraft Formation," AIAA Paper 1999-3143, June 1999.
- [12] Olwi, I., and Ghazi, M., "Effect of Wing Tip Vortices on Trailing Aircraft," *AIAA Journal*, Vol. 30, No. 9, 1992, pp. 2186–2187.  
doi:10.2514/3.11203
- [13] Stuijs, R., Jonville, G., Darracq, D., and Heinrich, R., "Inviscid Computation of Effect of Wake Vortices on a Scale-Model Airplane," *Journal of Aircraft*, Vol. 40, No. 1, Jan.–Feb. 2003, pp. 100–109.  
doi:10.2514/2.3063
- [14] Iannotta, B., "Vortex Draws Flight Research Forward," *Aerospace America*, Vol. 40, No. 3, March 2002, pp. 26–30.
- [15] Vachon, M. J., Ray, R. J., Walsh, K. R., and Ennix, K., "F/A-18 Aircraft Performance Benefits Measured During Autonomous Formation Flight Project," AIAA Paper 2002-4491, Aug. 2002.
- [16] Drinnon, R., "'Vortex Surfing' Could Be Revolutionary," United States Air Force [online database], <http://www.af.mil/news/story.asp?id=123321609> [retrieved 15 Oct. 2012].
- [17] Thuloweit, K., "Formation Flight System Keeps C-17s in Line," Edwards Air Force Base [online database], <http://www.edwards.af.mil/news/story.asp?id=123223228> [retrieved 23 Sept. 2010].
- [18] Giulietti, F., Innocenti, M., Napolitano, M., and Pollini, L., "Dynamics and Control Issues of Formation Flight," *Journal of Aerospace Science and Technology*, Vol. 9, No. 1, 2005, pp. 65–71.  
doi:10.1016/j.ast.2004.06.011
- [19] Campa, G., Gu, Y., Seanor, B., Napolitano, M. R., Pollini, L., and Fravolini, M. L., "Design and Flight-Testing of Non-Linear Formation Control Laws," *Journal of Control Engineering Practice*, Vol. 15, No. 9, 2007, pp. 1077–1092.  
doi:10.1016/j.conengprac.2007.01.004
- [20] Binetti, P., Ariyur, K. B., and Krstić, M., "Formation Flight Optimization Using Extremum Seeking Feedback," *Journal of Guidance, Control, and Dynamics*, Vol. 26, No. 1, 2003, pp. 132–142.  
doi:10.2514/2.5024
- [21] Chichka, D. F., Speyer, J. L., Fanti, C., and Park, C. G., "Peak-Seeking Control for Drag Reduction in Formation Flight," *Journal of Guidance, Control, and Dynamics*, Vol. 29, No. 5, Sept.–Oct. 2005, pp. 1221–1230.  
doi:10.2514/1.15424
- [22] Chichka, D. F., Wolfe, J. D., and Speyer, J. L., "Aerodynamically Coupled Formation Flight of Aircraft," *Proceedings of the 10th Mediterranean Conference on Control and Automation: MED2002* [CD-ROM], Instituto Superior Técnico, Lisbon, Portugal, 9–12 July 2002.
- [23] Ryan, J. J., and Speyer, J. L., "Peak-Seeking Control Using Gradient and Hessian Estimates," *Proceedings of the American Control Conference*, IEEE, Baltimore, MD, June 2010, pp. 611–616.
- [24] Bradley, S., Mursch–Radlgruber, E., and von Hünerbein, S., "Sodar Measurements of Wing Vortex Strength and Position," *Journal of Atmospheric and Oceanic Technology*, Vol. 24, No. 2, Feb. 2007, pp. 141–155.  
doi:10.1175/JTECH1966.1
- [25] Harris, M., Young, R. I., Köpp, F., Dolfi, A., and Cariou, J.-P., "Wake Vortex Detection and Monitoring," *Journal of Aerospace Science and Technology*, Vol. 6, No. 5, 2002, pp. 325–331.  
doi:10.1016/S1270-9638(02)01171-9
- [26] Rodenhiser, R. J., Durgin, W. W., and Johari, H., "Ultrasonic Method for Aircraft Wake Vortex Detection," *Journal of Aircraft*, Vol. 44, No. 3, 2007, pp. 726–732.  
doi:10.2514/1.25060
- [27] Rubin, W. L., "Radar-Acoustic Detection of Aircraft Wake Vortices," *Journal of Atmospheric and Oceanic Technology*, Vol. 17, No. 8, Aug. 2000, pp. 1058–1065.  
doi:10.1175/1520-0426(2000)017<1058:RADOAW>2.0.CO;2
- [28] Rutishauser, D., Lohr, G., Hamilton, D., Powers, R., McKissick, B., Adams, C., and Norris, E., "Wake Vortex Advisory System (WakeVAS) Concept of Operations," NASA TM-2003-212176, April 2003.
- [29] Smalikhov, I. N., and Rham, S., "Lidar Investigations of the Effects of Wind and Atmospheric Turbulence on an Aircraft Wake Vortex," *Journal of Atmospheric and Oceanic Optics*, Vol. 23, No. 2, 2010, pp. 137–146.  
doi:10.1134/S1024856010020107
- [30] Vicroy, D. D., Vijgen, P. M., Reimer, H. M., Gallegos, J. L., and Spalart, P. R., "Recent NASA Wake-Vortex Flight Tests, Flow-Physics Database and Wake-Development Analysis," AIAA Paper 1998-5592, 1998.
- [31] Fischenberg, D., "A Method to Validate Wake Vortex Encounter Models from Flight Data," International Congress of the Aeronautical Sciences Paper 2010-6.9.1, Sept. 2010.
- [32] Fischenberg, D., and Schwarz, C., "Wake Encounter In-Situ Flight Tests in Cruise–Wake Characterization," *4th Major WakeNet3-Europe Workshop* [online database], <http://www.wakenet.eu/index.php?id=185> [retrieved 1 March 2012].
- [33] Ide, K., and Ghil, M., "Extended Kalman Filtering for Vortex Systems, Part I: Methodology and Point Vortices," *Dynamics of Atmospheres and Oceans*, Vol. 27, Nos. 1–4, 1997, pp. 301–332.  
doi:10.1016/S0377-0265(97)00016-X
- [34] Ide, K., and Ghil, M., "Extended Kalman Filtering for Vortex Systems, Part II: Rankine Vortices and Observing-System Design," *Dynamics of Atmospheres and Oceans*, Vol. 27, Nos. 1–4, 1997, pp. 333–350.  
doi:10.1016/S0377-0265(97)00017-1
- [35] Kuznetsov, L., Ide, K., and Jones, C. K. R. T., "A Method for Assimilation of Lagrangian Data," *Monthly Weather Review*, Vol. 131, No. 10, 2003, pp. 2247–2260.  
doi:10.1175/1520-0493(2003)131<2247:AMFAOL>2.0.CO;2
- [36] Suzuki, T., and Colonius, T., "Inverse-Imaging Method for Detection of a Vortex in a Channel," *AIAA Journal*, Vol. 41, No. 9, 2003, pp. 1743–1751.  
doi:10.2514/2.7292
- [37] Moran, J., "Wings of Finite Span," *Introduction to Theoretical and Computational Aerodynamics*, Wiley, New York, 1984, pp. 124–148.
- [38] Katz, J., and Plotkin, A., "Three-Dimensional Numerical Solutions," *Low-Speed Aerodynamics*, 2nd ed., Cambridge Univ. Press, New York, 2001, pp. 331–368.
- [39] Jazwinski, A. H., "Approximate Nonlinear Filters," *Stochastic Processes and Filtering Theory*, Dover Publications, New York, 2007, pp. 332–365.
- [40] Speyer, J. L., and Chung, W. H., "Conditional Expectations and Discrete-Time Kalman Filtering," *Stochastic Processes, Estimation, and Control*, SIAM, Philadelphia, 2008, pp. 81–111.
- [41] Ristic, B., Arulampalam, S., and Gordon, N., "A Tutorial on Particle Filters," *Beyond the Kalman Filter: Particle Filters for Tracking Applications*, Artech House, Boston, 2004, pp. 35–62.